

Scalable quantum computing model in the circuit-QED lattice with circulator function

Mun Dae Kim · Jaewan Kim

Received: date / Accepted: date

Abstract We propose a model for a scalable quantum computing in the circuit-quantum electrodynamics(QED) architecture. In the Kagome lattice of qubits three qubits are connected to each other through a superconducting three-junction flux qubit at the vertices of the lattice. By controlling one of the three Josephson junction energies of the intervening flux qubit we can achieve the circulator function that couples arbitrary pair of two qubits among three. This selective coupling enables the interaction between two nearest neighbor qubits in the Kagome lattice, and further the two-qubit gate operation between any pair of qubits in the whole lattice by performing consecutive nearest neighbor two-qubit gates.

Keywords circuit quantum electrodynamics · circulator · scalable quantum computing

1 Introduction

Owing to the remarkable advancements in the qubit (quantum bit) coherence and control the scalable and programmable quantum computing is expected to be realized in the near future [1, 2, 3, 4, 5, 6, 7, 8, 9, 10, 11, 12, 13]. A large scale quantum computer consisting of many qubits integrated may perform quantum algorithms capable of carrying out tasks that are hard or impossible for ordinary classical computer. Such algorithms can accomplish, for example, factoring number of large digits [14] and searching a large data base [15]. These tasks require the controllability of coupling between two qubits in the scalable design, which is severely challenging. We, here, provide an approach to cope with this challenge by using the circuit-quantum electrodynamics (QED) architecture [16, 17].

Korea Institute for Advanced Study, Seoul 02455, Korea
E-mail: mdkim@kias.re.kr

In the circuit-QED scheme scalable designs for one-dimensional array [18, 19, 20, 21, 22, 23, 24] and two-dimensional lattice system [25, 26, 27, 28] have been proposed. There can be two possibilities to control the qubit-qubit interaction in scalable circuit-QED design. One is to control the resonator-resonator coupling by using an intervening dc-SQUID [28], flux qubit [37, 38, 39, 40], Josephson ring modulator [41], or transmon qubit [42]. On the other hand one can try to tune the coupling between qubit and transmission line resonator by controlling the qubit frequency [29, 30, 31, 32] or a coupling element inserted between qubit and resonator [33, 34, 35, 36].

For the universal quantum gate the two-qubit gate for an arbitrary pair of qubits among three is required. Hence we need the circulator function which enables selective coupling between arbitrary two resonators at the vertex point. Circulator is a nonreciprocal three-port device that routes a signal to the next port. Recently Josephson junction based microwave circulators have been proposed for the quantum information processing with superconducting devices [43, 44].

In this study we construct the Kagome lattice where three resonators are coupled at each vertex through an intervening three-Josephson junction flux qubit. The Josephson junction of the flux qubit consists of dc-SQUID loop whose effective Josephson junction energy can be controlled by threading a magnetic flux into the dc-SQUID loop. By reducing one of three effective Josephson junction energies we are able to achieve the microwave circulator function and to control *in situ* the sense of circulation. We couple qubits to the resonators and then the selective resonator coupling enables the two-qubit gate between an arbitrary pair of qubits among three. Further the quantum gate operation between arbitrary pair of qubits in the whole lattice can be achieved through consecutive two-qubit gates with switching function.

2 Coupling two circuit-QED cavities

First, for simplicity, we consider the case that only two resonators are coupled through a three-Josephson junction flux qubit as shown in Fig. 1(a). There are three trisection points in the coupling flux qubit, among which two resonators are connected to the flux qubit at two points A and B. We will study the case that all three resonators are coupled to the trisection points A, B and C later. Here dc-SQUID loops are introduced to control the effective Josephson coupling energy $E_{J_i} = E_J \cos(\pi\Phi_{si}/\Phi_0)$ with the Josephson coupling energy E_J of the junctions in the dc-SQUIDS and the superconducting unit flux quantum $\Phi_0 = h/2e$ by threading an external flux Φ_{si} into i -th dc-SQUID loop.

The periodic boundary condition around the flux qubit loop [45, 47] becomes $(1/3)(k'_1 + 2k'_2)L' = 2\pi(m + f_t) - \phi_1 - \phi_2 - \phi_3$, where m is an integer, k'_i the wave vector of the Cooper pair wavefunction in the flux qubit loop, ϕ_i the phase difference across the Josephson junction, L' the circumference of the loop, $f_t = f + f_{\text{ind}}$, $f = \Phi_x/\Phi_0$ and $f_{\text{ind}} = \Phi_{\text{ind}}/\Phi_0$ with the external magnetic flux Φ_x and the induced magnetic flux Φ_{ind} . The induced magnetic

flux is given by $\Phi_{\text{ind}} = L'_s(I'_1 + 2I'_2)/3$, where L'_s is the loop self inductance and $I'_i = -(n_c A q_c / m_c) \hbar k'_i$ is the loop current of the flux qubit, and thus we have $f_{\text{ind}} = -(L'_s / L'_K)(L'/3)(k'_1 + 2k'_2)/2\pi$. Here, $L'_K = m_c L' / A n_c q_c^2$ is the kinetic inductance [45], A the cross section of loop, $q_c = 2e$ and $m_c = 2m_e$.

Including the induced flux effect the periodic boundary condition is written as

$$\frac{1}{3} \left(1 + \frac{L'_s}{L'_k} \right) (k'_1 + 2k'_2) L' = 2\pi(m + f) - \phi_1 - \phi_2 - \phi_3. \quad (1)$$

Further we have the current conservation relations in Fig. 1(a) such that $I_1 = I'_1 - I'_2$ and $I_2 = I'_2 - I'_1$, that is, $k_1 = k'_1 - k'_2$ and $k_2 = k'_2 - k'_1$, and thus $k'_1 - k'_2 = (1/2)(k_1 - k_2)$, where $I_i = -(n_c A q_c / m_c) \hbar k_i$. On the other hand the current relation, $I'_i = -I_{ci} \sin \phi_i + C'_i \dot{V}_i$, of the capacitively-shunted model of Josephson junction can be represented as

$$-(n_c A q_c / m_c) \hbar k'_i = -I_{ci} \sin \phi_i - C'_i (\Phi_0 / 2\pi) \ddot{\phi}_i \quad (2)$$

by using the Josephson voltage-current relation $V_i = -(\Phi_0 / 2\pi) \dot{\phi}_i$ with C'_i being the capacitance of Josephson junction, n_c the Cooper pair density and $I_{ci} = 2\pi E_{Ji} / \Phi_0$ the critical current of Josephson junction.

From these relations we can obtain the equation of motion for the phase variable ϕ_j ,

$$\begin{aligned} \left(\frac{\Phi_0}{2\pi} \right)^2 C'_j \ddot{\phi}_j &= \frac{\Phi_0^2}{2(L'_s + L'_K)\pi} \left(m + f - \frac{1}{2\pi} \sum_{i=1}^3 \phi_i \right) \\ &\quad - E_{Jj} \sin \phi_j + p_j \frac{\Phi_0}{12\pi} (I_1 - I_2), \end{aligned} \quad (3)$$

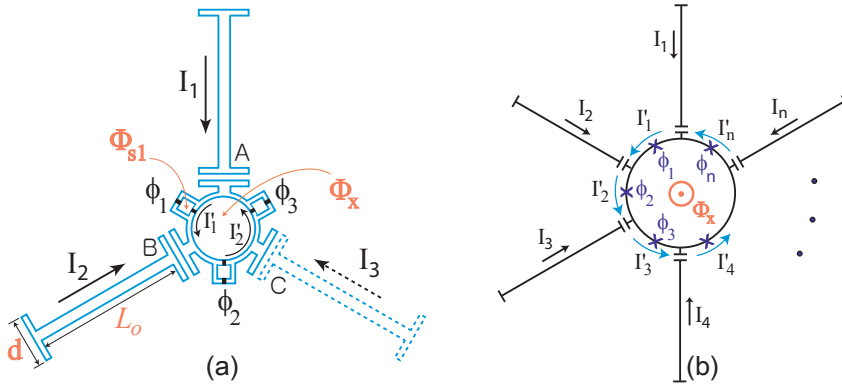


Fig. 1 (a) Schematic diagram for two resonators coupled via a three-junction flux qubit through an interface capacitance at the trisection points A and B. The flux Φ_{s_i} threading the dc-SQUID loop controls the effective Josephson coupling energy of the flux qubit and ϕ_i is the phase difference across the dc-SQUID. The flux threading the three-junction flux qubit loop is usually set as $\Phi_x = 0.5\Phi_0$. I_i is the current flowing from the resonator to the flux qubit loop through the capacitance, and I'_i is the current flowing in each segment of flux qubit loop. (b) n resonators are simultaneously coupled via an n -junction flux qubit loop, where each dc-SQUID is abbreviated as a single Josephson junction.

where $p_1 = -2$ and $p_2 = p_3 = 1$. This equation of motion can be derived from the Lagrange equation, $(d/dt)\partial\mathcal{L}/\partial\dot{\phi}_i - \partial\mathcal{L}/\partial\phi_i = 0$, with the Lagrangian

$$\mathcal{L}(\phi_i, \dot{\phi}_i) = \sum_{i=1}^3 \frac{1}{2} C'_i \left(\frac{\Phi_0}{2\pi} \right)^2 \dot{\phi}_i^2 - U_{\text{eff}}(\{\phi_i\}), \quad (4)$$

$$U_{\text{eff}}(\{\phi_i\}) = \frac{\Phi_0^2}{2(L'_s + L'_K)} \left(m + f - \frac{1}{2\pi} \sum_{i=1}^3 \phi_i \right)^2 + \sum_{i=1}^3 E_{Ji} (1 - \cos \phi_i) - \frac{\Phi_0}{12\pi} (I_1 - I_2) (\phi_2 + \phi_3 - 2\phi_1). \quad (5)$$

Hence we can consider this Lagrangian describes the dynamics of the system in Fig. 1(a).

For the usual parameter regime for the three-Josephson junction flux qubit [48] we can neglect L'_K because $L'_K/L'_s \sim 0.01$. Further, the inductive energy $\Phi_0^2/2L'_s$ dominates over the other energy scales so that the first term in Eq. (5) can be removed leaving the usual flux quantization condition, $2\pi(m + f) - \sum_{i=1}^3 \phi_i \approx 0$ at the minimum energy [49]. By using this constraint with $m = 0$ and introducing the coordinate $\phi_{\pm} = (\phi_2 \pm \phi_3)/2$ the effective potential can be transformed to

$$U_{\text{eff}}(\phi_+, \phi_-) \approx -E_{J1} \cos(2\pi f - 2\phi_+) - 2E_J \cos \phi_+ \cos \phi_- - \frac{\Phi_0}{6\pi} (I_1 - I_2) (-2\pi f + 3\phi_+), \quad (6)$$

where we consider that one junction has smaller Josephson coupling energy while two junctions larger one such that $E_{J1} < E_{J2} = E_{J3} = E_J$.

In Fig. 2(a) we show the effective potential $U_{\text{eff}}(\phi_+, \phi_-)$. If there is no current from resonators, $I_1 = I_2 = 0$, the effective potential $U_{\text{eff}}(\phi_+, \phi_-)$ has local minima along $\phi_- = 0$ and $\phi_+ = \alpha(-\alpha)$ with $\alpha = |\phi_{+, \text{min}}|$ at the local minima, corresponding to the counterclockwise (clockwise) current state, $|\downarrow\rangle$ ($|\uparrow\rangle$), of the flux qubit loop. In the tight-binding approximation the Hamiltonian can be written as $H = E_{\downarrow} |\downarrow\rangle\langle\downarrow| + E_{\uparrow} |\uparrow\rangle\langle\uparrow| - t_q (|\downarrow\rangle\langle\uparrow| + |\uparrow\rangle\langle\downarrow|)$ with t_q being the tunneling amplitude between the potential local minima when two states, $|\downarrow\rangle$ and $|\uparrow\rangle$, are degenerate, $E_{\downarrow} = E_{\uparrow}$. If a finite dc-bias current $I_1 - I_2$ is applied, the effective potential becomes tilted, whose profile along the dashed line in Fig. 2(a) is shown in Fig. 2(b). As a result, one of the two energy levels increases while the other decreases, and thus the degeneracy of the diagonal terms of the Hamiltonian H become broken such as $(E_{\downarrow} - \Phi_0\alpha(I_1 - I_2)/2\pi) |\downarrow\rangle\langle\downarrow| + (E_{\uparrow} + \Phi_0\alpha(I_1 - I_2)/2\pi) |\uparrow\rangle\langle\uparrow|$. Since $E_{J1} < E_{J2} = E_{J3} = E_J$ and the junction with larger Josephson coupling energy has a smaller phase difference, we have $\alpha \lesssim \pi/3$ and $\phi_2 = \phi_3$, *i.e.*, $\phi_- = 0$ at the potential minima in the central part of Fig. 2(b).

Consider two resonators are coupled to the intervening flux qubit loop at the end of the resonators as shown in Fig. 1(a). In the design we introduce a large capacitance between two line segments of length d through which the current flows between a resonator and the intervening qubit loop. In this

study we consider the second harmonic mode of resonator for later purpose. The second harmonic mode of current in j -th resonator can be represented as $\mathcal{I}_j(x, t) = -i\sqrt{\hbar\omega_{rj}/l_s L} \sin(2\pi x/L)[a_j(t) - a_j^\dagger(t)]$ [16,47] in terms of the boson operator $a_j(t)$ with ω_{rj} being the frequency of resonator mode, l_s the inductance density and $L = L_0 + d$ the effective length of resonator. Here, the origin of x -coordinate is at the center of resonator.

The charge fluctuation in the resonator induces the current flowing into the flux qubit loop given by $I_j(t) = \int_{L_0/2}^{L/2} \dot{q}_j(x, t) dx$ which can be represented by the difference of currents at both ends of the interface, $I_j(t) = \mathcal{I}_j(L/2, t) - \mathcal{I}_j(L_0/2, t)$ by using the current conservation $\dot{q}_j(x, t) = \partial \mathcal{I}_j(x, t) / \partial x$. Hence the current flowing from the j -th resonator can be written as

$$I_j(t) = -i\sqrt{\frac{\hbar\omega_{rj}}{l_s L}} \sin\left(\frac{\pi d}{L}\right) [a_j(t) - a_j^\dagger(t)]. \quad (7)$$

We can put this ac-current of resonator into the effective potential of Eq. (6), and then the total Hamiltonian is represented in the basis of $|0\rangle = (|\downarrow\rangle + |\uparrow\rangle)/\sqrt{2}$ and $|1\rangle = (|\downarrow\rangle - |\uparrow\rangle)/\sqrt{2}$ as follows:

$$\mathcal{H} = \hbar \sum_{j=1,2} \omega_{rj} a_j^\dagger a_j + \frac{1}{2} \omega_a \sigma_z + \frac{i}{2} g \sigma_x [(a_1 - a_1^\dagger) - (a_2 - a_2^\dagger)], \quad (8)$$

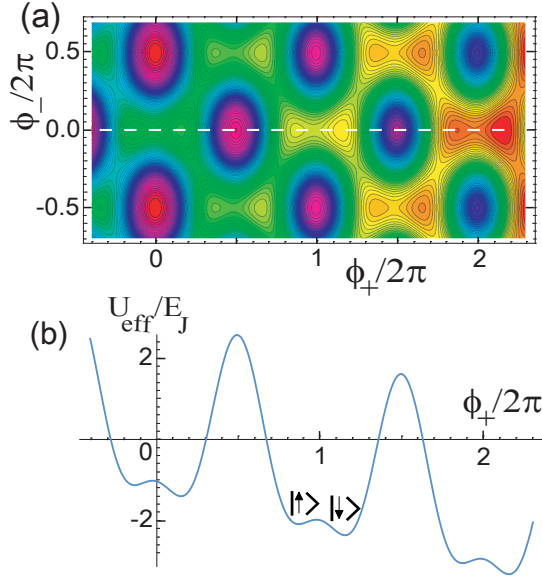


Fig. 2 (a) Effective potential $U_{\text{eff}}(\phi_+, \phi_-)$ of the coupled two-resonator system in Fig. 1(a). We set $(I_1 - I_2)/I_c = 0.05$, $f = 0.5$, and $E_{J1}/E_J = 0.8$. (b) Potential profile along the dashed line in (a). The resonator current $I_1 - I_2$ tilts the potential and thus the degeneracy of the current states, $|\uparrow\rangle$ and $|\downarrow\rangle$, is broken.

with the coupling strength $g \approx \alpha \Phi_0 \sqrt{\hbar \omega_r / l_s L} (d/L)$ and $\omega_a = 2t_q$, where we set $\omega_{rj} = \omega_r$. This Hamiltonian describes the interaction between the resonator modes 1 and 2. The last term of Hamiltonian \mathcal{H} shows that a photon in the resonator 1 excites the flux qubit state and then the flux qubit goes back to the ground state, generating a photon in resonator 2, and vice versa. Therefore, two resonators are coupled by using the flux qubit as an intervening qubit mediating the interaction [42].

3 Two-qubit gate in the Kagome lattice of qubits

Now we consider the case that all three trisection points A, B , and C are coupled to resonators in Fig. 1(a). Generally n resonators can be coupled to the intervening flux qubit as shown in Fig. 1(b). Then the periodic boundary condition around the flux qubit loop is given by $(L'/n) \sum_{i=1}^n k'_i = 2\pi(m+f) - \sum_{i=1}^n \phi_i$. From the relations $\Phi_{\text{ind}} = L'_s \sum_{i=1}^n I'_i/n$ and $I_i = -(n_c A q_c / m_c) \hbar k_i$, we have $f_{\text{ind}} = -(L'_s/L'_K)(L'/n) \sum_{i=1}^n k'_i/2\pi$, and thus

$$\left(1 + \frac{L'_s}{L'_K}\right) \sum_{i=1}^n k'_i \frac{L'}{n} = 2\pi(m+f) - \sum_{i=1}^n \phi_i. \quad (9)$$

By evaluating k'_i from this periodic boundary condition and the current conservation $I'_1 = I'_n + I_1, I'_2 = I'_1 + I_2, I'_3 = I'_2 + I_3, \dots, I'_n = I'_{n-1} + I_n$, that is, $k'_1 = k'_n + k_1, k'_2 = k'_1 + k_2, k'_3 = k'_2 + k_3, \dots, k'_n = k'_{n-1} + k_n$, and putting k'_i into the current relation of capacitively-shunted model of Josephson junction, $I'_i = -I_{ci} \sin \phi_i + C'_i \dot{V}_i$, we obtain an equation of motion for ϕ_j ,

$$\begin{aligned} \left(\frac{\Phi_0}{2\pi}\right)^2 C'_j \ddot{\phi}_j &= \frac{\Phi_0^2}{2(L'_s + L'_K)\pi} \left(m+f - \frac{1}{2\pi} \sum_{i=1}^n \phi_i\right) \\ &\quad - E_{Jj} \sin \phi_j + \frac{\Phi_0}{2\pi n} \sum_{i=1}^n ((n-i+j) \bmod n) I_i. \end{aligned} \quad (10)$$

This equation of motion can be obtained from the Lagrange equation with the effective potential

$$\begin{aligned} U_{\text{eff}}(\{\phi_i\}) &= \frac{\Phi_0^2}{2L'_s} \left(m+f - \frac{1}{2\pi} \sum_{i=1}^n \phi_i\right)^2 + \sum_{i=1}^n E_{Ji} (1 - \cos \phi_i) \\ &\quad - \frac{\Phi_0}{2\pi n} \sum_{i,j=1}^n ((n-i+j) \bmod n) \phi_j I_i. \end{aligned} \quad (11)$$

For $n = 3$, specifically, the last term of the effective potential $U_{\text{eff}}(\{\phi_i\})$ can be represented as $(\Phi_0/6\pi)[\phi_1(I_2 - I_3) + \phi_2(I_3 - I_1) + \phi_3(I_1 - I_2)]$. In Fig. 1(b) we consider that the junction with phase difference ϕ_1 has smaller Josephson coupling energy while two junctions larger one such that $E_{J1} < E_{J2} = E_{J3} = E_J$. Then, from the analysis similar to that in the previous

section with the boundary condition $\sum_{i=1}^3 \phi_i - 2\pi(m + f) = 0$ the effective potential $U_{\text{eff}}(\{\phi_i\})$ in Eq. (11) for $n = 3$ can be rewritten in the transformed coordinate $\phi_{\pm} = (\phi_2 \pm \phi_3)/2$ as

$$U_{\text{eff}}(\phi_+, \phi_-) = -E_{J1} \cos(2\pi f - 2\phi_+) - 2E_J \cos \phi_+ \cos \phi_- - \frac{\Phi_0}{6\pi} [(-2\pi f + 3\phi_+)(I_1 - I_2) + \phi_- (2I_3 - I_1 - I_2)]. \quad (12)$$

The sum of first two terms, which corresponds to the effective potential of the flux qubit, can have local minima for $\phi_- = 0$ as shown in Fig. 2(a). Here we set I_1 as the input bias current and I_2 and I_3 as the output current so that $I_1 = -I_2 - I_3$. The rms value of the resonator current is estimated as $I_{\text{rms}} = (1/\sqrt{2})\sqrt{\hbar\omega_{rj}/l_s L} = V_{\text{rms}}/Z \sim 20\text{nA}$, where the impedance of the resonator $Z = 50\Omega$ [36] and the $V_{\text{rms}} = E_{\text{rms}}b = 1\mu\text{V}$ with the electric field $E_{\text{rms}} = 0.2\text{V/m}$ and the distance $b = 5\mu\text{m}$ [17] between the transmission resonator and the ground plane. Then the amplitude of bias current in Eq. (7) becomes $|I_j| = 2\sqrt{\hbar\omega_{rj}/l_s L} \sin(\pi d/L) \approx 14\text{pA}$, where we set $L = 25\text{mm}$ and $d = 2\mu\text{m}$. Though the bias currents I_j are much smaller than the critical current of the flux qubit loop $I_c = 2\pi E_{J1}/\Phi_0 \sim 500\text{nA}$, the finite bias current may shift slightly the position of local minima of the total effective potential $U_{\text{eff}}(\phi_+, \phi_-)$.

In Fig. 3 we show the numerical result for a local minimum, $U_{\text{eff},\text{min}}(I_2)$, of the effective potential $U_{\text{eff}}(\phi_+, \phi_-)$ as a function of I_2/I_1 , where $\phi_{+,\text{min}} \approx \pi/3$ and $\phi_{-,\text{min}} \approx 0$ for $f = 0.5$ at the local minimum. Here the effective potential minimum decreases until the output current I_2 reaches the maximum

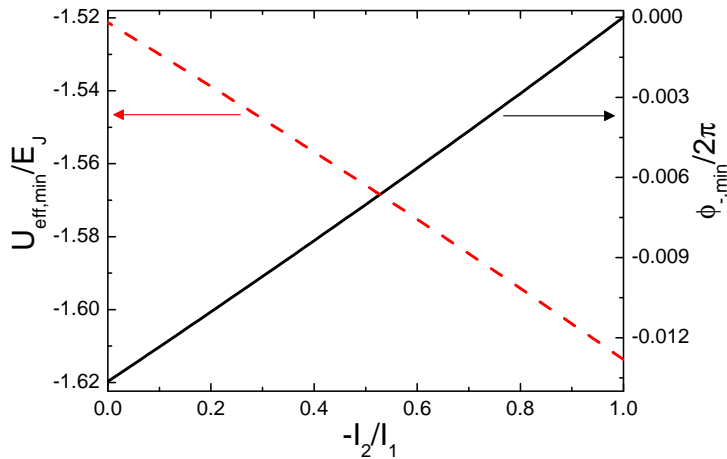


Fig. 3 The values of local minimum, $U_{\text{eff},\text{min}}$, of the effective potential $U_{\text{eff}}(\phi_+, \phi_-)$ around $\phi_+ \approx \pi/3$ and $\phi_- \approx 0$ for $f = 0.5$ (red dotted line) and ϕ_- at the local minimum, $\phi_{-,\text{min}}$, (black solid line) are shown as a function of I_2/I_1 .

value, $-I_1$, which can also be seen from the relation $\partial U_{\text{eff},\min}(I_2)/\partial I_2 = (\Phi_0/2\pi)(\phi_{+,\min} + \phi_{-,\min}) \approx \Phi_0/6 > 0$ with the effective potential in Eq. (12). This means that the input current I_1 from the $j = 1$ resonator flows through only $j = 2$ resonator ($I_2 = -I_1$) while there is no output current flowing through the $j = 3$ resonator ($I_3 = 0$).

As a result, at the local minimum the last term of the effective potential $U_{\text{eff}}(\phi_+, \phi_-)$ in Eq. (12) reduces to

$$-\frac{\Phi_0}{2\pi}\phi_{+,\min}(I_1 - I_2) \quad (13)$$

apart from the constant term independent of the phase variable ϕ_+ . This term shifts the value of $\phi_{+,\min}$, but we still have $\phi_{-,\min} = 0$ for $I_2 = -I_1$ at the local minimum of $U_{\text{eff}}(\phi_+, \phi_-)$ as shown in Fig. 3. Here, we leave the term, $I_1 - I_2$, in Eq. (13) which will be represented in boson operators, a_1 and a_2 , later. The condition $\phi_{-,\min} = 0$, i.e., $\phi_2 = \phi_3$ means that the currents $I'_i = -I_{ci} \sin \phi_i = -(2\pi E_{Ji}/\Phi_0) \sin \phi_i$ flowing across two junctions are equal to each other, $I'_2 = I'_3$, because $E_{J2} = E_{J3}$. Thus from the current conservation $I'_2 + I_3 = I'_3$ we have $I_3 = 0$. This is the reason why I_3 term in Eq. (12) disappears in Eq. (13). Therefore, by reducing one of the three Josephson junction energies with threading flux Φ_{si} we can determine the output current channel, which implements the current circulator function. Here the sense of circulation can be determined *in situ* by choosing a dc-SQUID loop to be threaded by the flux Φ_{si} .

The main decoherence of flux qubit comes from the flux fluctuation, δf . Though we consider $f = 0.5$ in Fig. 3, actually the relation $\partial U_{\text{eff},\min}(I_2)/\partial I_2 \approx \Phi_0/6 > 0$ is satisfied around $f \approx 0.5$. Hence, the value of $\phi_{-,\min} = 0$ in Fig. 3 is invariant and $I_2 = -I_1$ at the local minimum even in the presence of small flux fluctuations so that the circulator function may be robust against the flux noise.

Similarly to the two-resonator case the Hamiltonian in the tight-binding approximation can be written with the effective potential in Eq. (12) and the term in Eq. (13) as

$$H = E_{\downarrow}|\downarrow\rangle\langle\downarrow| + E_{\uparrow}|\uparrow\rangle\langle\uparrow| - t_q(|\downarrow\rangle\langle\uparrow| + |\uparrow\rangle\langle\downarrow|) - \frac{\Phi_0}{2\pi}\alpha(I_1 - I_2)(|\downarrow\rangle\langle\downarrow| - |\uparrow\rangle\langle\uparrow|), \quad (14)$$

where $\alpha = |\phi_{+,\min}|$. By using Eq. (7) this Hamiltonian can be transformed to

$$\mathcal{H} = \hbar \sum_{j=1}^3 \omega_{rj} a_j^\dagger a_j + \frac{1}{2} \omega_a \sigma_z + \frac{i}{2} g \sigma_x [(a_1 - a_1^\dagger) - (a_2 - a_2^\dagger)] \quad (15)$$

with $g \approx \alpha \Phi_0 \sqrt{\hbar \omega_r / l_s L} (d/L)$ in the basis of $|0\rangle$ and $|1\rangle$, where we set $\omega_{rj} = \omega_r$. The last term of this Hamiltonian enables a selective interaction between two resonators among three because there exists only the interaction between the current modes of $j = 1$ and $j = 2$ resonators other than $j = 3$.

If arbitrary one junction has a smaller Josephson junction energy in Fig. 1(b) for $n = 3$, the Hamiltonian is given by

$$\tilde{\mathcal{H}} = \hbar \sum_{j=1}^3 \omega_{rj} a_j^\dagger a_j + \frac{1}{2} \omega_a \sigma_z + \frac{i}{2} g \sigma_x [(a_l - a_l^\dagger) - (a_m - a_m^\dagger)], \quad (16)$$

where $(l, m) = (1, 2)$ if the smaller Josephson junction energy is E_{J1} . If the smaller Josephson junction energy is E_{J2} or E_{J3} , $(l, m) = (2, 3)$ or $(3, 1)$, respectively. Here, the chirality of the indices (l, m) originates from the direction of the threading external flux Φ_x . This Hamiltonian shows that only two resonators, (l, m) , interact with each other while the other resonator does not participate in the process. Hence one can decide the output channel for a given input, and select two-resonator interaction.

For the general case of n resonators connected at a vertex we consider that the k -th Josephson junction energy is smaller than others such that $E_{Jk} < E_{Ji}$ ($i \neq k$). With the flux quantization condition $\phi_k = 2\pi f - \sum_{i=1, i \neq k}^n \phi_i$ the condition $\partial U_{\text{eff}}(\{\phi_i\}) / \partial \phi_i = 0$ for extremal point results in $\phi_i = \phi$ for all i ($i \neq k$) at the potential minima. Then the last term of the effective potential

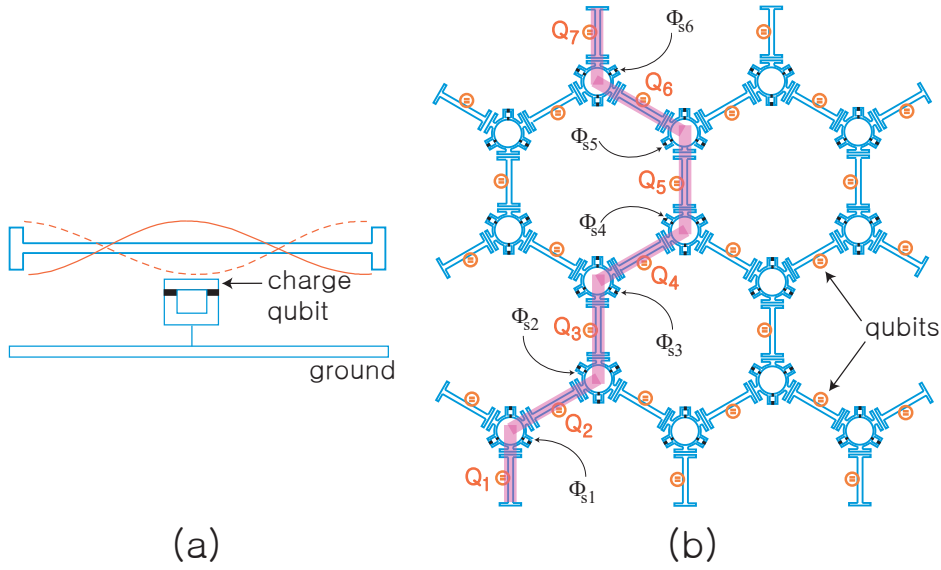


Fig. 4 (a) Circuit-QED architecture with a qubit coupled to a transmission line resonator. Here, we consider a superconducting charge qubit capacitively coupled to the resonator. (b) Two-dimensional lattice based on the model for coupling resonators in Fig. 1(b) for $n = 3$, where qubits coupled with the resonators form the Kagome lattice. Pair of interacting qubits can be chosen by threading a flux Φ_{s_i} into the dc-SQUID between the two corresponding resonators.

$U_{\text{eff}}(\{\phi_i\})$ in Eq. (11) becomes

$$-\frac{\Phi_0}{4\pi}\phi\sum_{i=1}^n[n-1-2((n-i+k)\bmod n)]I_i. \quad (17)$$

When $n = 3$ and $k = 1$, we can recover the result in Eq. (13) which describes the interaction between two resonators. For $n > 3$, however, this term contains more than two currents I_i and thus we cannot obtain two resonator interaction any more. Hence in order to achieve interaction between arbitrary two resonators connected to the same vertex we should consider $n = 3$ case.

In order to describe the quantum gate operation between two qubits we introduce a qubit coupled to a resonator as shown in Fig. 4(a). Here, we consider, for example, a superconducting charge qubit capacitively coupled at the center of the superconducting transmission line resonator through the second harmonic voltage mode of resonator [16]. In Fig. 4(b) qubits Q_i are introduced at each resonator of the lattice for $n = 3$, where we can perform a quantum gate operation between arbitrary two qubits among three qubits connected at a vertex of a lattice. These qubits interact with each other through the resonator-resonator coupling. Among three qubits connected at a vertex arbitrary pair of two qubits can interact with each other by threading a magnetic flux Φ_{si} into the dc-SQUID between the two resonators coupled with the qubits.

By extending the structure for $n = 3$ we can have a lattice structure in two-dimensional space as shown in Fig. 4(b). The intervening flux qubits form the hexagonal lattice, but the qubits coupled to the resonators form the Kagome lattice. Two qubits Q_1 and Q_2 , for example, can interact with each other by threading the flux Φ_{s1} , and then two qubits Q_2 and Q_3 can interact with each other by threading the flux Φ_{s2} after switching off the coupling between qubits Q_1 and Q_2 . Switch-off can be done by threading a flux Φ_x far away from $0.5\Phi_0$ into the intervening flux qubit between qubits Q_1 and Q_2 . In this way arbitrary series of two-qubit gates with qubits, for example, $Q_1 \cdots Q_7$ can be performed in the Kagome lattice shown in Fig. 4. As a result, we can achieve the effective interaction between two remote qubits, Q_1 and Q_7 , which is the key ingredient for the scalable quantum computing.

4 Conclusion

We have proposed a model for a scalable quantum computing in the Kagome lattice based on the circuit-QED architecture. By controlling the flux threading one of the three dc-SQUID loops of intervening flux qubit the circulator function has been implemented in the superconducting circuit. Hence we can control *in situ* the sense of circulation, which is a key ingredient in the microwave quantum technology. A scalable quantum computing requires the selective interaction between two qubits among many qubits coupled at a vertex point of the qubit lattice. In this study, we have shown that by using the circulator function we can perform the selective two-qubit gate for the case

that only three qubits are coupled at the vertex through an intervening qubit, where the qubit sites form the Kagome lattice. When more than three qubits are coupled at a vertex, we have shown that the selective two-qubit coupling cannot be achieved.

The two-qubit interaction between remote qubits are crucial for the scalable quantum computing. In our design we can perform the selective two-qubit gate between nearest neighbor qubits. Thus by performing these two-qubit gates consecutively with switching function we would achieve the quantum gate operation between arbitrary pair of qubits in the lattice. We also have discussed that the circulator function in this paper is robust against the flux fluctuations, which will enable the experimental realization of present scalable quantum computing model.

Acknowledgements This work was partly supported by the KIST Institutional Program (Project No. 2E26680-16-P025) and by Basic Science Research Program through the National Research Foundation of Korea (NRF) funded by the Ministry of Education, Science and Technology (2011-0023467).

References

1. I. A. Silva et al., Phys. Rev. Lett. 117, 160402 (2016).
2. A. Streltsov, G. Adesso, and M. B. Plenio, arXiv:1609.02439.
3. Z.-X. Man, Y.-J. Xia, and R. Lo Franco, Sci. Rep. 5, 13843 (2015); Phys. Rev. A 92, 012315 (2015).
4. T. R. Bromley, M. Cianciaruso, R. Lo Franco, and G. Adesso, J. Phys. A 47, 405302 (2014); M. Cianciaruso, T. R. Bromley, W. Roga, R. Lo Franco, and G. Adesso, Sci. Rep. 5, 10177 (2015).
5. V. Vedral, Nature Phys. 10, 256 (2014).
6. N. Brunner, D. Cavalcanti, S. Pironio, V. Scarani, and S. Wehner, Rev. Mod. Phys. 86, 419 (2014).
7. K. Modi, A. Brodutch, H. Cable, T. Paterek, and V. Vedral, Rev. Mod. Phys. 84, 1655 (2012).
8. P. Haikka, T. H. Johnson, and S. Maniscalco, Phys. Rev. A 87, 010103(R) (2013).
9. R. Lo Franco, New J. Phys. 17, 081004 (2015).
10. A. Orioux et al., Sci. Rep. 5, 8575 (2015).
11. A. D'Arrigo, R. Lo Francod, G. Benentia, E. Paladinob, and G. Falcib, Ann. Phys. 350, 211 (2014).
12. A. Mortezapour, M. A. Borji, and R. Lo Franco, Laser Phys. Lett. 14, 055201 (2017).
13. B. Aaronson, R. Lo Franco, and G. Adesso, Phys. Rev. A 88, 012120 (2013); B. Aaronson, R. Lo Franco, G. Compagno, and G. Adesso, New J. Phys. 15, 093022 (2013).
14. P. W. Shor, SIAM J. Comput. 26, 1484 (1997).
15. L. K. Grover, Phys. Rev. Lett. 79, 4709 (1997).
16. A. Blais, R.-S. Huang, A. Wallraff, S. M. Girvin, and R. J. Schoelkopf, Phys. Rev. A 69, 062320 (2004).
17. A. Blais, J. Gambetta, A. Wallraff, D. I. Schuster, S. M. Girvin, M. H. Devoret, and R. J. Schoelkopf, Phys. Rev. A 75, 032329 (2007).
18. P. Nataf and C. Ciuti, Phys. Rev. Lett. 104, 023601 (2010).
19. L. Tian, Phys. Rev. Lett. 105, 167001 (2010).
20. M. Leib and M. J. Hartmann, New J. Phys. 12, 093031 (2010).
21. M. Leib, F. Deppe, A. Marx, R. Gross, and M. J. Hartmann, New J. Phys. 14, 075024 (2012).
22. O. Viehmann, J. von Delft, and F. Marquardt, Phys. Rev. Lett. 110, 030601 (2013).
23. A. Kurcz, A. Bermudez, and J. J. García-Ripoll, Phys. Rev. Lett. 112, 180405 (2014).

24. J. Raftery, D. Sadri, S. Schmidt, H. E. Türeci, and A. A. Houck, *Phys. Rev. X* **4**, 031043 (2014).
25. A. A. Houck, H. E. Türeci, and J. Koch, *Nature Phys.* **8**, 292 (2012).
26. D. L. Underwood, W. E. Shanks, J. Koch, and A. A. Houck, *Phys. Rev. A* **86**, 023837 (2012).
27. S. Schmidt and J. Koch, *Ann. Phys.* **525**, 395 (2013).
28. B. Peropadre, D. Zueco, F. Wulschner, F. Deppe, A. Marx, R. Gross, and J. J. Garcia-Ripoll, *Phys. Rev. B* **87**, 134504 (2013).
29. J. Majer, J. M. Chow, J. M. Gambetta, J. Koch, B. R. Johnson, J. A. Schreier, L. Frunzio, D. I. Schuster, A. A. Houck, A. Wallraff, A. Blais, M. H. Devoret, S. M. Girvin, and R. J. Schoelkopf, *Nature* **449**, 443 (2007).
30. L. DiCarlo, J. M. Chow, J. M. Gambetta, L. S. Bishop, B. R. Johnson, D. I. Schuster, J. Majer, A. Blais, L. Frunzio, S. M. Girvin, and R. J. Schoelkopf, *Nature* **460**, 240 (2009).
31. L. DiCarlo, M. D. Reed, L. Sun, B. R. Johnson, J. M. Chow, J. M. Gambetta, L. Frunzio, S. M. Girvin, M. H. Devoret, and R. J. Schoelkopf, *Nature* **467**, 574 (2010).
32. L. Steffen, Y. Salathe, M. Oppliger, P. Kurpiers, M. Baur, C. Lang, C. Eichler, G. Puebla-Hellmann, A. Fedorov, and A. Wallraff, *Nature* **500**, 319 (2013).
33. B. Peropadre, P. Forn-Díaz, E. Solano, and J. J. García-Ripoll, *Phys. Rev. Lett.* **105**, 023601 (2010).
34. G. Romero, D. Ballester, Y. M. Wang, V. Scarani, and E. Solano, *Phys. Rev. Lett.* **108**, 120501 (2012).
35. M. S. Allman, J. D. Whittaker, M. Castellanos-Beltran, K. Cicak, F. da Silva, M. P. DeFeo, F. Lecocq, A. Sirois, J. D. Teufel, J. Aumentado, and R. W. Simmonds, *Phys. Rev. Lett.* **112**, 123601 (2014).
36. M. D. Kim, *Quantum Inf. Process.* **14**, 3677 (2015).
37. M. Mariani, F. Deppe, A. Marx, R. Gross, F. K. Wilhelm, and E. Solano, *Phys. Rev. B* **78**, 104508 (2008).
38. G. M. Reuther, D. Zueco, F. Deppe, E. Hoffmann, E. P. Menzel, T. Weißl, M. Mariani, S. Kohler, A. Marx, E. Solano, R. Gross, and P. Hanggi, *Phys. Rev. B* **81**, 144510 (2010).
39. A. Baust, E. Hoffmann, M. Haeberlein, M. J. Schwarz, P. Eder, J. Goetz, F. Wulschner, E. Xie, L. Zhong, F. Quijandria, B. Peropadre, D. Zueco, J. J. Garcia Ripoll, E. Solano, K. Fedorov, E. P. Menzel, F. Deppe, A. Marx, and R. Gross, *Phys. Rev. B* **91**, 014515 (2015).
40. F. Wulschner, J. Goetz, F. R. Koessel, E. Hoffmann, A. Baust, P. Eder, M. Fischer, M. Haeberlein, M. J. Schwarz, M. Pernpeintner, E. Xie, L. Zhong, C. W. Zollitsch, B. Peropadre, J. J. Garcia Ripoll, E. Solano, K. Fedorov, E. P. Menzel, F. Deppe, A. Marx, R. Gross, arXiv:1508.06758.
41. E. Flurin, N. Roch, J. D. Pillet, F. Mallet, and B. Huard, *Phys. Rev. Lett.* **114**, 090503 (2015).
42. M. D. Kim and J. Kim, *Phys. Rev. A* **93**, 012321 (2016).
43. J. Koch, A. A. Houck, K. Le Hur, and S. M. Girvin, *Phys. Rev. A* **82**, 043811 (2010).
44. K. M. Sliwa, M. Hatridge, A. Narla, S. Shankar, L. Frunzio, R. J. Schoelkopf, and M. H. Devoret, *Phys. Rev. X* **5**, 041020 (2015).
45. M. D. Kim, D. Shin, and J. Hong, *Phys. Rev. B* **68**, 134513 (2003).
46. M. D. Kim and J. Hong, *Phys. Rev. B* **70**, 184525 (2004).
47. M. D. Kim and K. Moon, *J. Korean Phys. Soc.* **58**, 1599 (2011); arXiv:1005.1703.
48. I. Chiorescu, Y. Nakamura, C. J. P. M. Harmans and J. E. Mooij, *Science* **299**, 1869 (2003).
49. T. P. Orlando, J. E. Mooij, L. Tian, C. H. van der Wal, L. S. Levitov, Seth Lloyd, and J. J. Mazo, *Phys. Rev. B* **60**, 15398 (1999).